Efficient Angle Estimation for MIMO Systems via Redundancy Reduction Representation

Zhang, Yu; Wang, Yue; Tian, Zhi; Leus, Geert; Zhang, Gong

DOI
10.1109/LSP.2022.3164850

Publication date
2022

Document Version
Final published version

Published in
IEEE Signal Processing Letters

Efficient Angle Estimation for MIMO Systems via Redundancy Reduction Representation

Yu Zhang, *Member, IEEE*, Yue Wang, *Senior Member, IEEE*, Zhi Tian, *Fellow, IEEE*, Geert Leus, *Fellow, IEEE*, and Gong Zhang, *Member, IEEE*

***Abstract*—This paper proposes an efficient direction of departure (DOD) and direction of arrival (DOA) estimation method for multi-input multi-output (MIMO) systems. For uncorrelated scenarios, the redundancy of the covariance matrix is first exploited by establishing its concise representation through redundancy reduction, which transforms the original large-size covariance matrix into a smaller-size matrix without loss of useful angle information. Then, the resulting transformed matrix, which retains a salient structure, permits efficient two-dimensional (2D) angle estimators working on a reduced-size problem for DOD and DOA estimation. Compared with conventional subspace-based methods, the proposed method incorporating an appropriate 2D angle estimator is more computationally efficient and can achieve higher estimation accuracy for small numbers of snapshots and low signal-to-noise ratios, which are verified by simulation results.**

***Index Terms*—DOD and DOA estimation, MIMO systems, redundancy reduction representation, transformation matrix construction.**

I. Introduction

Direction of departure (DOD) and direction of arrival (DOA) estimation plays an important role in parameter estimation for multi-input multi-output (MIMO) systems, where two-dimensional (2D) subspace-based angle estimation algorithms are applied [1]–[10]. For example, ESPRIT [3] and 2D-MUSIC [4], as two representative algorithms, have been widely employed. However, to implement 2D-MUSIC, a 2D spectral peak searching is required, at a cost of an expensively high computation load. To overcome this disadvantage, an efficient reduced-dimension MUSIC (RD-MUSIC) [5] has been developed by dividing the simultaneous 2D spectral peak search into separate one dimensional (1D) angle estimators. The RD-MUSIC, as an efficient modification of 2D-MUSIC, still belongs to the class of subspace-based algorithms. For RD-MUSIC, an eigenvalue decomposition (EVD) on the covariance matrix of the observations is still required similar to ESPRIT and 2D-MUSIC. The EVD operation results in a computational complexity that is cubic in the product of the numbers of transmitters and receivers in the MIMO system denoted by N and M, respectively, which can be computationally expensive as N and/or M go large [11].

In this paper, an efficient angle estimation method is proposed for MIMO systems, by exploring a potential redundancy structure hidden in the 2D covariance and exploiting it to derive a transformation from the covariance to its core matrix which enables a new design of 2D estimators for angle estimation. In doing so, the main contributions of this letter are summarized as follows: 1) a redundancy reduction representation of the 2D covariance matrix is first proposed by exploiting its redundancy structure; 2) based on such a redundancy reduction representation, an efficient linear construction from the original large covariance to its concise core matrix is then derived in a closed-form expression, which is parameterized by its dimensions N and M only; 3) 2D angle estimators are developed over the core matrix for DOD and DOA estimation. Different from standard subspace-based methods where EVD operations are always required, the proposed method relies on a simple linear transformation only. Further, thanks to the sparsity nature of the transformation matrix, such a linear transformation can be applied in a computation-efficient manner. As a result, the proposed method is more efficient than its subspace-based counterparts. Simulation results demonstrate the efficiency and effectiveness of the proposed method.

Notations: a, $\boldsymbol{a}$ and $\boldsymbol{A}$ denote a scalar, a vector and a matrix, respectively. $(\cdot)^T$, $(\cdot)^*$, and $(\cdot)^H$ are the transpose, conjugate, and conjugate transpose of a vector or matrix. $\text{diag}(\boldsymbol{a})$ generates a diagonal matrix with the diagonal elements constructed from $\boldsymbol{a}$. $\text{vec}(\cdot)$ stacks all the columns of a matrix into a vector and $\text{vec}^{-1}(\cdot)$ is the inverse operation of $\text{vec}(\cdot)$. $\boldsymbol{e}_a$ and $\boldsymbol{q}_a$ are the vectors with only the a-th element being one and zeros elsewhere. $\boldsymbol{I}_a$ is an a-size identity matrix and $\boldsymbol{K}_a$ is an a-size anti-diagonal identity matrix. $\boldsymbol{A}^\dagger$ is the pseudoinverse of $\boldsymbol{A}$. $\otimes$ is the Kronecker product. $\odot$ is the Khatri-Rao product. $\mathbb{E}\{\cdot\}$ denotes expectation.

Manuscript received March 7, 2022; accepted March 27, 2022. Date of publication April 5, 2022; date of current version May 3, 2022. This work was supported in part by the U.S. National Science Foundation (NSF) under Grants 1527396, 1939553, 2003211, 2128596, and 2136202; in part by the Virginia Research Investment Fund CCI under Grant 223996; in part by the NSF of China (NSFC) under Grants 61871218 and 61801211; in part by the Fundamental Research Funds for the Central University under Grant 3082017NP2017421; in part by the Open Research Fund of the Key Lab of Radar Imaging and Microwave Photonics under Grant NJ20210001; and in part by the ASPIRE Project under Grant 14926 through the OTP program of NWO-TTW. The associate editor coordinating the review of this manuscript and approving it for publication was Dr. Luis Antonio Azpicueta-Ruiz. *(Corresponding author: Yu Zhang.)*

Yu Zhang and Gong Zhang are with the Key Lab of Radar Imaging and Microwave Photonics, Ministry of Education, Nanjing University of Aeronautics and Astronautics, Nanjing 211100, China (e-mail: skywalker_zy@163.com; gzhang@nuaa.edu.cn).

Yue Wang and Zhi Tian are with the Department of Electrical and Computer Engineering, George Mason University, Fairfax, VA 22030 USA (e-mail: ywang56@gmu.edu; ztian1@gmu.edu).

Geert Leus is with the Faculty of Electrical Engineering, Mathematics and Computer Science, Delft University of Technology, 2826 Delft, The Netherlands (e-mail: g.j.t.leus@tudelft.nl).

Digital Object Identifier 10.1109/LSP.2022.3164850

II. Problem Formulation

Consider a MIMO system equipped with uniform linear arrays (ULA) at both its transmit and receive base stations, where N and M antennas are spaced with half-wavelength, respectively. This MIMO system can be either a MIMO communications system [8], [9] or a bistatic MIMO radar system [10]. Assume that there are K uncorrelated targets or channel paths for the bistatic MIMO radar system or the MIMO communications system, respectively. Assuming orthogonal transmit waveforms, the output of the matched filters at the receiver contaminated by noise can be expressed as [5]

$$\begin{aligned}\boldsymbol{y}(t) &= \boldsymbol{x}(t) + \boldsymbol{n}(t)\\ &= \sum_{k=1}^{K} s_k(t)\boldsymbol{a}_r(\theta_k) \otimes \boldsymbol{a}_t(\phi_k) + \boldsymbol{n}(t)\\ &= \boldsymbol{A}_r(\boldsymbol{\theta}) \odot \boldsymbol{A}_t(\boldsymbol{\phi})\boldsymbol{s}(t) + \boldsymbol{n}(t),\ \ t = 1, \ldots, L, \quad (1)\end{aligned}$$

where $s_k(t)$ is the radar cross section complex coefficient of the k-th target for bistatic MIMO radar systems or the path gain of the k-th channel path for MIMO communications systems. L is the number of collected snapshots. The receive and transmit steering vector $\boldsymbol{a}_r(\theta_k)$ and $\boldsymbol{a}_t(\phi_k)$ of size M and N are of the form

$$\begin{aligned}\boldsymbol{a}_r(\theta_k) &= [1, e^{-j\pi\sin(\theta_k)}, \ldots, e^{-j\pi(M-1)\sin(\theta_k)}]^T\\ \boldsymbol{a}_t(\phi_k) &= [1, e^{-j\pi\sin(\phi_k)}, \ldots, e^{-j\pi(N-1)\sin(\phi_k)}]^T, \quad (2)\end{aligned}$$

where θ_k and ϕ_k are the corresponding DOA and DOD of the k-th target/path with respect to the receive array normal and transmit array normal, respectively. $\boldsymbol{n}(t)$ is the additive Gaussian white noise vector satisfying $\mathcal{N}(\boldsymbol{0}, \sigma^2\boldsymbol{I}_{MN})$. And, $\boldsymbol{s}(t) = [s_1(t), \ldots, s_K(t)]^T$, $\boldsymbol{\theta} = [\theta_1, \ldots, \theta_K]^T$, $\boldsymbol{\phi} = [\phi_1, \ldots, \phi_K]^T$, $\boldsymbol{A}_r(\boldsymbol{\theta}) = [\boldsymbol{a}_r(\theta_1), \ldots, \boldsymbol{a}_r(\theta_K)]$ and $\boldsymbol{A}_t(\boldsymbol{\phi}) = [\boldsymbol{a}_t(\phi_1), \ldots, \boldsymbol{a}_t(\phi_K)]$.

Given $\boldsymbol{y}(t)$ collected from (1), the covariance matrix of the observation is

$$\begin{aligned}\boldsymbol{R}_y &= \mathbb{E}\{\boldsymbol{y}(t)\boldsymbol{y}^H(t)\} = \boldsymbol{R}_x + \sigma^2\boldsymbol{I}_{MN}\\ &= \sum_{k=1}^{K} r_k(\boldsymbol{a}_r(\theta_k)\otimes\boldsymbol{a}_t(\phi_k))(\boldsymbol{a}_r(\theta_k)\otimes\boldsymbol{a}_t(\phi_k))^H + \sigma^2\boldsymbol{I}_{MN}\\ &= (\boldsymbol{A}_r(\boldsymbol{\theta}) \odot \boldsymbol{A}_t(\boldsymbol{\phi}))\boldsymbol{R}_s(\boldsymbol{A}_r(\boldsymbol{\theta}) \odot \boldsymbol{A}_t(\boldsymbol{\phi}))^H + \sigma^2\boldsymbol{I}_{MN}, \quad (3)\end{aligned}$$

where

$$\boldsymbol{R}_x = (\boldsymbol{A}_r(\boldsymbol{\theta}) \odot \boldsymbol{A}_t(\boldsymbol{\phi}))\boldsymbol{R}_s(\boldsymbol{A}_r(\boldsymbol{\theta}) \odot \boldsymbol{A}_t(\boldsymbol{\phi}))^H \quad (4)$$

is the noise-free covariance matrix with $\boldsymbol{R}_s = \mathrm{diag}(r_1, \ldots, r_K) \succeq 0$ being a diagonal positive semidefinite matrix. In practical applications, $\boldsymbol{R}_y$ is estimated over L collected snapshots through $\hat{\boldsymbol{R}}_y = \frac{1}{L}\sum_{t=1}^{L}\boldsymbol{y}(t)\boldsymbol{y}^H(t)$.

The goal of 2D angle estimation in this letter is to recover the unknown DOD and DOA pairs $\{\phi_k, \theta_k\}_k$ from $\hat{\boldsymbol{R}}_y$.

III. Proposed Method

This section proposes an efficient 2D angle estimation method for MIMO systems. In doing so, we first develop a redundancy reduction representation of the covariance matrix by exploiting the redundancy of the covariance matrix. Then, a transformation matrix is constructed as a linear mapping which transforms the original large-size covariance matrix into a smaller-size core matrix without losing any useful information. Finally, 2D angle estimation is developed over such a smaller-size core matrix.

A. Redundancy Reduction Representation

By vectorizing (3), we have

$$\mathrm{vec}(\boldsymbol{R}_y) = \mathrm{vec}(\boldsymbol{R}_x) + \sigma^2\mathrm{vec}(\boldsymbol{I}_{MN}). \quad (5)$$

Based on (4) and the diagonal feature of $\boldsymbol{R}_s$, the first term on the right hand side of (5) can be expressed as

$$\mathrm{vec}(\boldsymbol{R}_x) = \sum_{k=1}^{K} r_k(\boldsymbol{a}_r^*(\theta_k) \otimes \boldsymbol{a}_t^*(\phi_k)) \otimes (\boldsymbol{a}_r(\theta_k) \otimes \boldsymbol{a}_t(\phi_k)). \quad (6)$$

The key innovation is now to rewrite the basic term in (6) as

$$\begin{aligned}&(\boldsymbol{a}_r^*(\theta_k) \otimes \boldsymbol{a}_t^*(\phi_i)) \otimes (\boldsymbol{a}_r(\theta_k) \otimes \boldsymbol{a}_t(\phi_k))\\ &= \boldsymbol{\Psi}(\boldsymbol{a}'_r(\theta_k) \otimes \boldsymbol{a}'_t(\phi_k)), \quad (7)\end{aligned}$$

where $\boldsymbol{a}'_r(\theta_k) \in \mathbb{C}^{2M-1}$ and $\boldsymbol{a}'_t(\phi_k) \in \mathbb{C}^{2N-1}$ are given by

$$\begin{aligned}\boldsymbol{a}'_r(\theta_k) &= [e^{-j\pi(M-1)\sin(\theta_k)}, \ldots, 1, \ldots, e^{j\pi(M-1)\sin(\theta_k)}]^T,\\ \boldsymbol{a}'_t(\phi_k) &= [e^{-j\pi(N-1)\sin(\phi_k)}, \ldots, 1, \ldots, e^{j\pi(N-1)\sin(\phi_k)}]^T. \quad (8)\end{aligned}$$

The tall matrix

$$\boldsymbol{\Psi} = (\boldsymbol{I}_M \otimes \boldsymbol{E} \otimes \boldsymbol{I}_N)(\boldsymbol{G}_M \otimes \boldsymbol{G}_N) \in \mathbb{C}^{M^2N^2 \times (2M-1)(2N-1)} \quad (9)$$

is defined as a redundancy-reduction representation matrix that is determined by N and M only, where $\boldsymbol{E} = \sum_{j=1}^{N}(\boldsymbol{e}_j^T \otimes \boldsymbol{I}_M \otimes \boldsymbol{e}_j) \in \mathbb{C}^{NM \times NM}$ with $\boldsymbol{e}_j \in \mathbb{C}^N$ is the commutation matrix, $\boldsymbol{G}_M$ is defined as

$$\boldsymbol{G}_M = \left[\boldsymbol{G}_{M,1}^T, \ldots, \boldsymbol{G}_{M,M}^T\right]^T \in \mathbb{C}^{M^2 \times (2M-1)}, \quad (10)$$

with the i-th block matrix $\boldsymbol{G}_{M,i} = [\boldsymbol{0}_{M \times (M-i)}, \boldsymbol{K}_M, \boldsymbol{0}_{M \times (i-1)}]$, $i = 1, \ldots, M$, and $\boldsymbol{G}_N \in \mathbb{C}^{N^2 \times (2N-1)}$ is defined similarly as (10). Substituting (7) into (6), we have

$$\begin{aligned}\mathrm{vec}(\boldsymbol{R}_x) &= \boldsymbol{\Psi}\sum_{k=1}^{K} r_k\boldsymbol{a}'_r(\theta_k) \otimes \boldsymbol{a}'_t(\phi_k)\\ &= \boldsymbol{\Psi}\mathrm{vec}(\boldsymbol{A}'_t(\boldsymbol{\phi})\boldsymbol{R}_s\boldsymbol{A}'^T_r(\boldsymbol{\theta})) = \boldsymbol{\Psi}\mathrm{vec}(\boldsymbol{Z}), \quad (11)\end{aligned}$$

where $\boldsymbol{Z}$ is called the core matrix of the original covariance $\boldsymbol{R}_x$ in this letter. We have $\boldsymbol{Z} = \boldsymbol{A}'_t(\boldsymbol{\phi})\boldsymbol{R}_s\boldsymbol{A}'^T_r(\boldsymbol{\theta}) \in \mathbb{C}^{(2N-1)\times(2M-1)}$ with $\boldsymbol{A}'_t(\boldsymbol{\phi}) = [\boldsymbol{a}'_t(\phi_1), \ldots, \boldsymbol{a}'_t(\phi_K)]$ and $\boldsymbol{A}'_r(\boldsymbol{\theta}) = [\boldsymbol{a}'_r(\theta_1), \ldots, \boldsymbol{a}'_r(\theta_K)]$. Moreover, the second term on the right hand side of (5) can be written as

$$\sigma^2\mathrm{vec}(\boldsymbol{I}_{MN}) = \sigma^2\boldsymbol{\Psi}\mathrm{vec}(\boldsymbol{Q}), \quad (12)$$

where $\boldsymbol{Q} = \boldsymbol{q}_N\boldsymbol{q}_M^T$ with $\boldsymbol{q}_N \in \mathbb{C}^{2N-1}$ and $\boldsymbol{q}_M \in \mathbb{C}^{2M-1}$. Hence, substituting (11) and (12) into (5), we have

$$\mathrm{vec}(\boldsymbol{R}_y) = \boldsymbol{\Psi}\mathrm{vec}(\boldsymbol{Z} + \sigma^2\boldsymbol{Q}). \quad (13)$$

According to (11), note that $\boldsymbol{Z}$ not only has a smaller size than $\boldsymbol{R}_x$, but also contains all the 2D angle information which is decoupled along its rows and columns. Therefore, we can efficiently retrieve the unknown angles from $\boldsymbol{Z}$ once $\boldsymbol{Z}$ is obtained. Now, the task boils down to obtaining an estimate of $\boldsymbol{Z}$ from $\hat{\boldsymbol{R}}_y$.

B. Transformation Matrix Construction

In fact, the linear projection from vec$(\boldsymbol{Z}+\sigma^2\boldsymbol{Q})$ to vec$(\boldsymbol{R}_y)$ in (13) is an injective mapping. Hence, the representation matrix $\boldsymbol{\Psi}$ is a full column rank matrix, which allows to rewrite (13) through the pseudoinverse of $\boldsymbol{\Psi}$ as

$$\text{vec}(\boldsymbol{Z}+\sigma^2\boldsymbol{Q}) = \boldsymbol{\Psi}^\dagger \text{vec}(\boldsymbol{R}_y) = \boldsymbol{T}\text{vec}(\boldsymbol{R}_y), \tag{14}$$

where $\boldsymbol{T} = \boldsymbol{\Psi}^\dagger \in \mathbb{C}^{(2M-1)(2N-1)\times M^2N^2}$ is the transformation matrix satisfying

$$\boldsymbol{T}\boldsymbol{\Psi} = \boldsymbol{I}_{(2M-1)(2N-1)}. \tag{15}$$

Next, we point out that besides making a detour to obtain $\boldsymbol{T}$ from $\boldsymbol{\Psi}$, $\boldsymbol{T}$ can be directly constructed based on several small-size sparse matrices with known M and N, which is more computation-efficient.

One of the properties of the commutation matrix [12] is

$$\boldsymbol{E}^T\boldsymbol{E} = \boldsymbol{I}_{MN}. \tag{16}$$

Further, the definitions of $\boldsymbol{G}_M$ and $\boldsymbol{G}_N$ in (10) lead to [11]

$$\begin{aligned} \boldsymbol{G}_M^T\boldsymbol{G}_M &= \boldsymbol{W}_M = \text{diag}([1,\ldots,M-1,M,M-1,\ldots,1]); \\ \boldsymbol{G}_N^T\boldsymbol{G}_N &= \boldsymbol{W}_N = \text{diag}([1,\ldots,N-1,N,N-1,\ldots,1]). \end{aligned} \tag{17}$$

Hence, we have

$$\begin{aligned} (\boldsymbol{I}_M\otimes\boldsymbol{E}^T\otimes\boldsymbol{I}_N)(\boldsymbol{I}_M\otimes\boldsymbol{E}\otimes\boldsymbol{I}_N) &= \boldsymbol{I}_{M^2N^2} \\ ((\boldsymbol{W}_M^{-1}\boldsymbol{G}_M^T)\otimes(\boldsymbol{W}_N^{-1}\boldsymbol{G}_N^T))(\boldsymbol{G}_M\otimes\boldsymbol{G}_N) &= \boldsymbol{I}_{(2M-1)(2N-1)}. \end{aligned} \tag{18}$$

Combining (9), (15) and (18), we have

$$\boldsymbol{T} = ((\boldsymbol{W}_M^{-1}\boldsymbol{G}_M^T)\otimes(\boldsymbol{W}_N^{-1}\boldsymbol{G}_N^T))(\boldsymbol{I}_M\otimes\boldsymbol{E}^T\otimes\boldsymbol{I}_N). \tag{19}$$

Hence, with $\boldsymbol{T}$ in (19), $\boldsymbol{Z}$ can be obtained from (14) as

$$\boldsymbol{Z} = \text{vec}^{-1}(\boldsymbol{T}\text{vec}(\boldsymbol{R}_y)) - \sigma^2\boldsymbol{Q}. \tag{20}$$

Moreover, considering the covariance matrix at hand is the sample covariance $\hat{\boldsymbol{R}}_y$ and the effect of the unknown noise term can be igored, the estimate of $\boldsymbol{Z}$ can be approximately obtained from (20) as

$$\hat{\boldsymbol{Z}} = \text{vec}^{-1}(\boldsymbol{T}\text{vec}(\hat{\boldsymbol{R}}_y)). \tag{21}$$

C. Angle Estimation

Note that the transformed smaller-size $\boldsymbol{Z}$ has a salient structure. Specifically,

$$\boldsymbol{Z} = \boldsymbol{A}_t'(\boldsymbol{\phi})\boldsymbol{R}_s\boldsymbol{A}_r'^T(\boldsymbol{\theta}) \tag{22}$$

can be regarded as a cross-correlation matrix collected from a virtual cross array with $\boldsymbol{A}_t'(\boldsymbol{\phi})$, $\boldsymbol{A}_r'^*(\boldsymbol{\theta})$ and $\boldsymbol{R}_s$ being the two manifold matrices and signal correlation matrix. By now, we transform the original problem of DOD and DOA estimation from the covariance matrix $\boldsymbol{R}_y$ for MIMO systems to a smaller-size problem of 2D DOA estimation from the core matrix $\boldsymbol{Z}$ also known as a cross-correlation matrix for an equivalent cross array [13], [14]. While the literature about angle estimation algorithms for cross arrays is limited, in this letter, we adopt the cross-correlation based algorithms for an L-shaped array [15]–[21] for 2D angle estimation since their cross-correlation matrices have similar structures. Hence, we develop a two-step method. In the first step, we obtain the estimate of $\boldsymbol{Z}$ from the sample covariance $\hat{\boldsymbol{R}}_y$ via (21). Then, in the second step, 2D angle estimators for L-shaped arryas can be employed with the obtained $\boldsymbol{Z}$ for DOD and DOA estimation. Moreover, to guarantee the proposed method has the unique solution, we have $K\leq 2\min\{M,N\}-2$. In other words, the largest detectable number is $2\min\{M,N\}-2$.

It is worth noting that with different 2D angle estimators, the resulting two-step algorithms will generally have distinct behaviors in terms of the estimation accuracy and computational complexity. Specifically, with an appropriate 2D angle estimator, e.g., the ESPRIT-like algorithm [16], the resulting redundancy reduction based ESPRIT (RR-ESPRIT) is one of the most efficient compared with traditional subspace-based methods, which will be verified in the next section.

TABLE I
THE COMPUTATIONAL COMPLEXITY OF DIFFERENT ALGORITHMS

Algorithm	Computational Complexity	Highest Order
2D-MUSIC	$\mathcal{O}\{LM^2N^2+M^3N^3+n^2[MN(MN-K)+MN-K]\}$	M^3N^3
RD-MUSIC	$\mathcal{O}\{LM^2N^2+M^3N^3+n[(M^2N+M^2)(NM-K)+M^2]\}$	M^3N^3
ESPRIT	$\mathcal{O}\{LM^2N^2+M^3N^3+2K^2(M-1)N+2K^2(N-1)M+6K^3\}$	M^3N^3
Proposed	$\mathcal{O}\{LM^2N^2+M^2N^2+80(2M-2)^3+2K^3\}$	M^2N^2

IV. COMPUTATIONAL COMPLEXITY

In this section, we analyze the computational complexity of the proposed RR-ESPRIT compared with the traditional 2D-MUSIC, RD-MUSIC and ESPRIT algorithms. Note that the transformation matrix $\boldsymbol{T}$ is only determined by M and N and can be constructed offline via (19). Moreover, according to (19), there is only one non-zero element in every column of $\boldsymbol{T}$. In other words, $\boldsymbol{T}$ is a sparse matrix with only M^2N^2 nonzero elements. Hence, the transformation in (21) produces a computation load of only $\mathcal{O}(M^2N^2)$. Other main computational costs of the RR-ESPRIT come from the sample covariance construction and the ESPRIT-like algorithm. The total computational complexity of the RR-ESPRIT compared with that of the 2D-MUSIC, RD-MUSIC and ESPRIT is listed in Table I, where n is the number of searching steps for the spectral peak search.

From Table I, note that the first summands of all the methods are the same, which represent the complexity of the sample covariance construction. The second summands of the three subspace-based methods describe the complexity of the EVD, while that of the proposed method is the complexity of the sparse matrix multiplication, followed by the complexity of the specific angle retrieval algorithms. Fig. 1 presents the computational complexity of the different algorithms versus the number of antennas at each base station with $L=10$, $K=3$ and $n=$

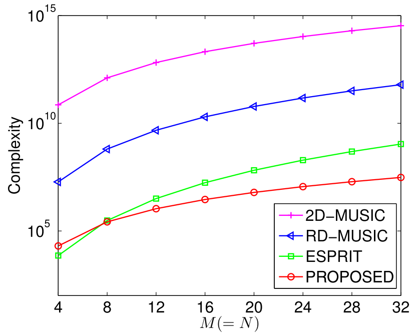

Fig. 1. The computational complexity of different algorithms versus M ($N = M$) with $L = 10$, $K = 3$ and $n = 18000$.

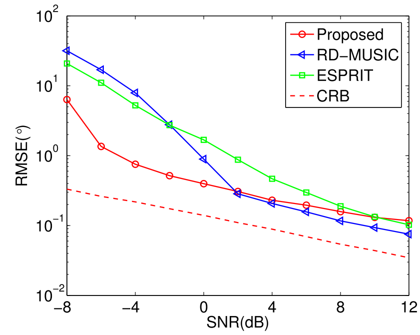

Fig. 2. Angle estimation RMSE versus SNR with $L = 10$.

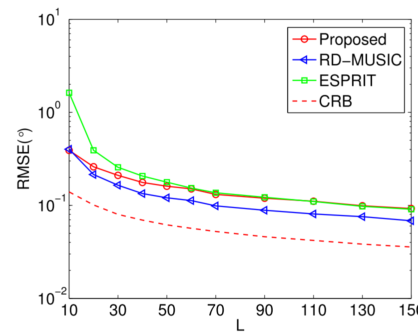

Fig. 3. Angle estimation RMSE versus Snapshots with SNR $= 0$ dB.

18000. As shown in Fig. 1, the curves of the subspace-based methods have similar slopes with different scaling. In contrast, the proposed method has a more gradual slope. That is because, with the growth of M and N, the second summands of the computational complexity order as in Table I are $\mathcal{O}(M^3N^3)$ and $\mathcal{O}(M^2N^2)$ for the subspace-based methods and the proposed method respectively, which contribute the main computation. Moreover, compared with the subspace-based methods, the proposed RR-ESPRIT becomes the most efficient one when the numbers of antennas $(N = M)$ go large, e.g., $M \geq 8$. Hence, given the recovered $\hat{\boldsymbol{Z}}$ from (21), it is important to choose a proper 2D angle estimator, e.g., the ESRPIT-like. The resulting algorithm yields an efficient angle estimation method especially with large M and/or N.

V. Simulation Results

This section presents the numerical results to evaluate the DOD and DOA estimation performance of the proposed method for MIMO systems. The root mean squared error (RMSE) is used to measure the estimation accuracy as RMSE $= \frac{1}{K}\sum_{k=1}^{K}(\frac{1}{M_t}\sum_{n=1}^{M_t}((\widetilde{\theta}_{k,n}-\theta_k)^2+(\widetilde{\phi}_{k,n}-\phi_k)^2))^{\frac{1}{2}}$, where M_t, $\widetilde{\theta}_{k,n}$ and $\widetilde{\phi}_{k,n}$ respectively denote the number of Monte-Carlo trials, and the estimates of θ_k and ϕ_k in the n-th experiment. The RR-ESPRIT algorithm is employed as the proposed method, while the conventional subspace-based algorithms such as ESPRIT [3] and RD-MUSIC [5] as well as the CRB [6] are depicted as benchmarks. We omit the 2D-MUSIC in simulations since it has a similar performance as RD-MUSIC but at a higher computational complexity [5]. As the same settings applied in Fig. 1, the angle search step size for the RD-MUSIC is set to $0.01°$, i.e., $n = 18000$. In simulations, a bistatic MIMO radar system with $M = N = 14$ is adopted. We also consider there are three equal power uncorrelated targets ($K = 3$) located at $(\phi_1, \theta_1) = (10°, 15°)$, $(\phi_2, \theta_2) = (20°, 25°)$ and $(\phi_3, \theta_3) = (30°, 35°)$.

First, Fig. 2 shows the RMSE of the aforementioned algorithms versus the SNR with $L = 10$. The figure shows that the proposed RR-ESPRIT outperforms ESPRIT and RD-MUSIC at low SNRs, e.g., SNR ≤ 2. This is because, with the transformation in (21), the estimation error between $\hat{\boldsymbol{R}}_y$ and $\boldsymbol{R}_y$ is averaged, which leads to error elimination to a certain extent. Although the RD-MUSIC has the best estimation performance at high SNRs, it consumes the highest computational cost from Fig. 1. Moreover, the proposed RR-ESPRIT is the most efficient one among these algorithms. Hence, the RR-ESPRIT is a nice alternative to the subspace-based methods at low SNRs.

Further, the RMSE of the aforementioned algorithms versus the number of snapshots is presented in Fig. 3. As shown in Fig. 3, the proposed RR-ESPRIT can even work better than the others with very few snapshots, $L = 10$. Moreover, the RR-ESPRIT outperforms the ESPRIT at a small number of snapshots, e.g., $L \leq 110$. Hence, the RR-ESPRIT is not only more computationally efficient, but also achieves a better estimation performance than other counterparts when the number of snapshots is small. Therefore, the proposed method with an appropriate 2D angle estimator is a nice alternative to the traditional subspace-based methods when N and/or M go large, especially at low SNRs and small numbers of snapshots.

VI. Conclusion

In this paper, an efficient DOD and DOA estimation method is proposed for MIMO systems. Given the sample covariance matrix, we first establish a redundancy reduction representation to represent the large-size covariance matrix by its smaller-size core matrix. Next, a transformation matrix that depicts the linear mapping from the covariance to its core matrix is constructed via several simple and sparse composition matrices. Finally, an efficient 2D angle estimator is developed by exploiting the salient structure of the transformed smaller-size core matrix, which benefits from a lower computational complexity and can achieve a better accuracy at low SNRs and small numbers of snapshots, compared with traditional subspace-based methods.

REFERENCES

[1] H. Yan, J. Li, and G. Liao, "Multitarget identification and localization using bistatic MIMO radar systems," *EURASIP J. Adv. Signal Process.*, vol. 2008, pp. 1–8, 2007.

[2] D. Chen, B. Chen, and G. Qin, "Angle estimation using ESPRIT in MIMO radar," *Electron. Lett.*, vol. 44, no. 12, pp. 770–771, 2008.

[3] J. Chen, H. Gu, and W. Su, "Angle estimation using ESPRIT without pairing in MIMO radar," *Electron. Lett.*, vol. 44, no. 24, pp. 1422–1423, 2008.

[4] X. Gao, X. Zhang, G. Feng, Z. Wang, and D. Xu, "On the MUSIC-derived approaches of angle estimation for bistatic MIMO radar," in *Proc. IEEE Int. Conf. Wireless Netw. Inf. Syst.*, 2009, pp. 343–346.

[5] X. Zhang, L. Xu, L. Xu, and D. Xu, "Direction of departure (DOD) and direction of arrival (DOA) estimation in MIMO radar with reduced-dimension MUSIC," *IEEE Commun. Lett.*, vol. 14, no. 12, pp. 1161–1163, Dec. 2010.

[6] X. Zhang and D. Xu, "Angle estimation in bistatic MIMO radar using improved reduced dimension capon algorithm," *J. Syst. Eng. Electron.*, vol. 24, no. 1, pp. 84–89, 2013.

[7] J. Xu, G. Liao, S. Zhu, L. Huang, and H. C. So, "Joint range and angle estimation using MIMO radar with frequency diverse array," *IEEE Trans. Signal Process.*, vol. 63, no. 13, pp. 3396–3410, Jul. 2015.

[8] Y. Wang, Y. Zhang, Z. Tian, G. Leus, and G. Zhang, "Super-resolution channel estimation for arbitrary arrays in hybrid millimeter-wave massive MIMO systems," *IEEE J. Sel. Topics Signal Process.*, vol. 13, no. 5, pp. 947–960, Sep. 2019.

[9] Y. Wang, Z. Tian, and X. Cheng, "Enabling technologies for spectrum and energy efficient NOMA-mmWave-maMIMO systems," *IEEE Wireless Commun.*, vol. 27, no. 5, pp. 53–59, Oct. 2020.

[10] Y. Wang, L. Zhang, and Z. Song, "Angle estimation of weak scatterers using improved MUSIC for bistatic MIMO radar," *IEEE Signal Process. Lett.*, vol. 27, pp. 2164–2167, 2020.

[11] Y. Zhang, G. Zhang, and X. Wang, "Computationally efficient DOA estimation for monostatic MIMO radar based on covariance matrix reconstruction," *Electron. Lett.*, vol. 53, no. 2, pp. 111–113, 2016.

[12] X.-D. Zhang, *Matrix Analysis and Applications*. Cambridge, U.K.: Cambridge Univ. Press, 2017.

[13] M. Carlin, P. Rocca, G. Oliveri, and A. Massa, "Bayesian compressive sensing as applied to directions-of-arrival estimation in planar arrays," *J. Elect. Comput. Eng.*, vol. 2013, pp. 1–12, 2013.

[14] F. Zhang, A. Jin, and Y. Hu, "Two-dimensional DOA estimation of MIMO radar coherent source based on Toeplitz matrix set reconstruction," *Secur. Commun. Netw.*, vol. 2021, pp. 1–9, 2021.

[15] J.-F. Gu and P. Wei, "Joint SVD of two cross-correlation matrices to achieve automatic pairing in 2-D angle estimation problems," *IEEE Antennas Wireless Propag. Lett.*, vol. 6, pp. 553–556, 2007.

[16] X. Zhang, X. Gao, and W. Chen, "Improved blind 2D-direction of arrival estimation with l-shaped array using shift invariance property," *J. Electromagn. Waves Appl.*, vol. 23, no. 5-6, pp. 593–606, 2009.

[17] G. Wang, J. Xin, N. Zheng, and A. Sano, "Computationally efficient subspace-based method for two-dimensional direction estimation with L-shaped array," *IEEE Trans. Signal Process.*, vol. 59, no. 7, pp. 3197–3212, Jul. 2011.

[18] X. Nie and L. Li, "A computationally efficient subspace algorithm for 2-D DOA estimation with L-shaped array," *IEEE Signal Process. Lett.*, vol. 21, no. 8, pp. 971–974, Aug. 2014.

[19] Y.-Y. Dong, C.-X. Dong, W. Liu, H. Chen, and G.-Q. Zhao, "2-D DOA estimation for L-shaped array with array aperture and snapshots extension techniques," *IEEE Signal Process. Lett.*, vol. 24, no. 4, pp. 495–499, Apr. 2017.

[20] M. Liu, H. Cao, and Y. Wu, "Improved subspace-based method for 2D DOA estimation with L-shaped array," *Electron. Lett.*, vol. 56, no. 8, pp. 402–405, 2020.

[21] Y. Zhang, Y. Sun, G. Zhang, X. Wang, and Y. Tao, "Crosscorrelation and DOA estimation for L-shaped array via decoupled atomic norm minimization," *Wireless Commun. Mobile Comput.*, vol. 2021, pp. 1–11, 2021.